Optical Axis Identification Technique for Free Space Optics Transmission

Yuki Tashiro, Yuta Shimada, Kiyotaka Izumi, Takeshi Tsujimura and Koichi Yoshida

***Abstract*—This paper describes optical axis adjustment technique for an active free space optics transmission system. This system precisely controls the direction of a collimated thin laser beam using a motor driven laser emitting mechanism and positioning photodiodes. Before beginning laser beam feedback control, it is required to guide the laser beam within the range of the positioning photodiodes for initial laser beam alignment. This paper proposes an arrival position presumption method of laser beam traveling along the long distance from transmitter. A positioning sensor containing several photodiodes measures laser luminescence distribution, and analytically calculates the optical axis of laser beam according to the modified Gaussian beam optics based on four or five distributed local intensity of laser luminescence. Experiments are conducted to evaluate the accuracy of the presumption, and results reveal that the method is effective in leading the laser beam onto a distant receiver.**

***Keywords*—alignmen, feedback control, free space optics (FSO), Gaussian beam optics, laser, opticel axis.**

I. Introduction

Free space optics (FSO) is an alternative telecommunication technology to optical fiber transmission or wireless local area network (LAN). It contains an optical- electrical (O/E) and an electrical-optical (E/O) converter to transmit and receive a laser beam through the air [1]. FSO system can be constructed easier and costlier than optical fiber network. It is securer than wireless LAN system from phone tapping as a collimated laser beam is exclusively transferred to the destination. Conventional FSO has been considered non-ubiquitous telecommunication technology because it is designed as a point-to-point communication [2]-[6]. FSO device is rigidly fixed to sturdy structure preventing tremors due to weather or traffic. Another weak point of conventional FSO is susceptible to disturbance against aerial laser transmission. Transmission is interrupted by a tiny obstacle that interferes a line-of-sight of the laser beam.

Free space optics system has developed to apply in various fields. Free space optical transmission is assorted in terms of transmission length into inter-chip transmission [7], indoor communication [8], inter-building network [9], last-mile access network [10], or satellite communication [11] as well as real systems such as telecommunication switching system, transportation communication and so on [12]-[14]. Aerial laser transmission technologies are investigated to improve the free space transmission performance from every possible aspect. More than 10 Gbps bandwidth of FSO laser transmission is realized by wavelength division multiplex (WDM) technology [15]-[17]. Aerial laser beam transmission suffers from optical characteristics of atmosphere. Thus some papers report on the countermeasures against disturbance by fog or scintillation [18]-[22]. Hybrid transmission systems are proposed which combines infrared laser with visible light [23], [24] or radio frequency [25], [26]. As one of the most important issues is alignment of optical axes of laser beam and receiver lens, a number of papers propose methods to adjust the laser beam direction and to increase coupling efficiency [27]-[29].

The authors have proposed active FSO technology to establish an optical mesh network that serves as a rural area network. It realizes ubiquitous broadband communication in the user network using direct optical coupling technique with a single-mode fiber and a free space optics system [30]. We also improved it to the switching system for non-interruptive optical fiber line and the optical alignment technique for free space optics systems [31]-[34]. That system directly emits the laser beam, which is transferred through fiber optics, in the air. It also controls the direction of laser beam using motor-driven reflection mirrors. The laser beam is managed to reach the receiver by feedback control to keep communication even when the FSO transmission suffers some disturbances. The control system is valid as far as the laser beam arrives within the view of laser positioning sensor.

We are adapting it to practical application fields such as long transmission beyond a river or between hilltops. One of the realistic problems is how to introduce the laser beam within the adjustable view to align the laser beam axis with a receiver. The authors have studied a laser beam adjustment system and conducted experiments to presume the optical axis of the arrived laser beam. The authors propose the design of the laser beam adjustment system, and deduces the formula of the optical axis based on Gaussian beam optics with regard to both centrosymmetric and axial-symmetric sensitivity of photodiodes (PDs). We evaluate the performance of optical axis presumption based on laser intensity distribution.

This paper describes design of the proposed laser transmission system in Section II. Section III details the principle of laser optical axis identification and some experimental results. Section IV concludes our study.

Manuscript received November 11, 2016; revised July 25, 2017.

Y. Tashido, Y. Shimada, K. Izumi, T. Tsujimura are with the Department of Mechanical Engineering, Graduate School of Science and Engineering, Saga University, Saga-city, 840-8502 Japan, e-mail: tujimura@cc.saga-u.ac.jp.

K. Yoshida is with Dept. of Information and Systems Engineering, Fukuoka Institute of Technology, Fukuoka-city, 811-0295 Japan.

This work was partially supported by Strategic Information and Communications RD Promotion Programme (SCOPE) of Ministry of Internal Affairs and Communications, Japan.

doi: 10.11601/ijates.v6i2.213

II. Laser Transmission System

A wired/wireless hybrid optical network is contrived by installing an FSO system within a commercial optical fiber transmission line. It is equipped with collimator lenses at the end of optical fiber cables to convert optical signals through the optical fiber to an aerial laser beam. An FSO system focuses the laser beam on 10 m core in the optical fiber through the collimator lens.

Figure 1 expresses the block diagram of full duplex active FSO system, where two FSO terminals symmetrically transmit laser beam. This active FSO system contains a transmitter, a receiver, and a controller PC. It tracks a tremoring receiver maintaining broadband communication by means of the laser tracking feature. Positioning error of laser beam is measured by the dedicated sensor in the opposite FSO apparatus, and that information is transferred through the upstream transmission laser beam traveling from the opposite transmitter. The feed-back control data is delivered and superimposed on the optical signals carrying communication data. Two planer position sensitive detectors (PSD) catch positional and angular errors, respectively. Measured data is acquired by the controller PC through analog-to-digital (A/D) converter to create control commands. Galvanic scanners and a 2 degree of freedom (DOF) tilting mirror are steered to reduce those errors.

Figure 2 illustrates a laser beam transmission of the proposed active free space optics system that transmits 1 Gbps bilateral laser signals. An optical signal is sent into the transmitter through an optical fiber at first. It is discharged from a collimator lens in the air, and reflected on the mirrors toward the receiver. The control system steers the emitted laser beam accurately onto the receiver. Five positioning photodiodes surrounding the receiver measure the distribution of laser intensity to estimate positioning error of the arrived laser beam. The beam direction is adjusted by feedback control of the transmitter according to the error estimation.

We designed the active free space optics transmitter illustrated in Fig. 3. The laser beam travels from the opposite transmitter, and reflects on galvanic scanner mirrors and a tilting mirror. It is divided by a beam splitter and finally reaches both the receiver and PSDs. Then we actually constructed a prototype as shown in Fig. 4. The transmitter is equipped with two direct current (DC) servo motors and a piezo-driven 2DOF actuator to control mirrors reflecting laser beam at an arbitrary position and angle. This prototype is successful in tracking the receiver travelling at 320 mm/s in an accuracy of 1 mm, while the transmitter is 5 m apart from the target. This system can be available more than 1000 m apart in principle, because the actuators can rotate mirrors in an accuracy of 0.5 x 10^{-6} rad.

We have also designed the dedicated positioning photodiode set which is composed of several photodiodes to detect local power of laser wavelength. Four photodiodes surround the transmission photodiode as shown in Fig. 5. They are not concerned in communication but only in measurement of intensity of laser luminescence.

The transmitter of prototyped laser transmission system is equipped with a fiber-optic collimator, FH10-NIR-FC (New-

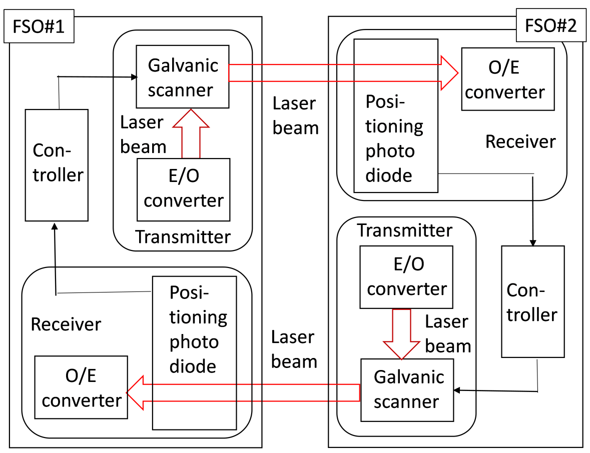

Fig. 1. Full duplex active FSO system.

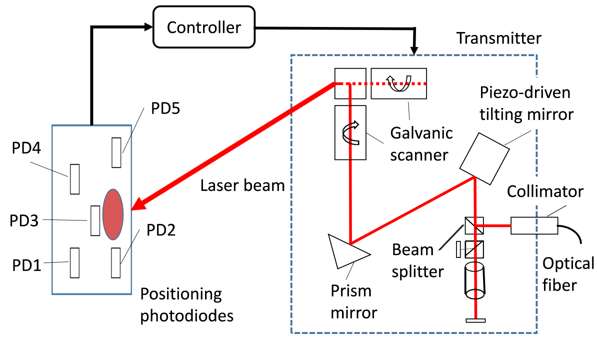

Fig. 2. Active free space optics system.

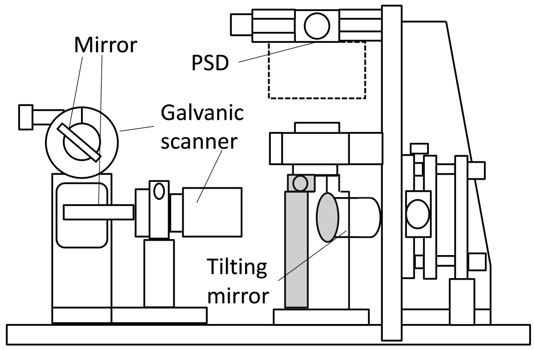

Fig. 3. FSO transmitter design.

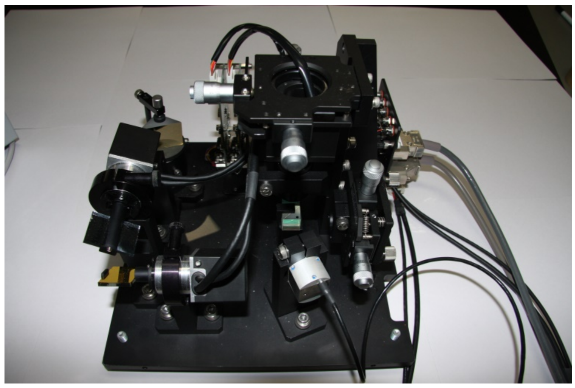

Fig. 4. Prototyped FSO transmitter.

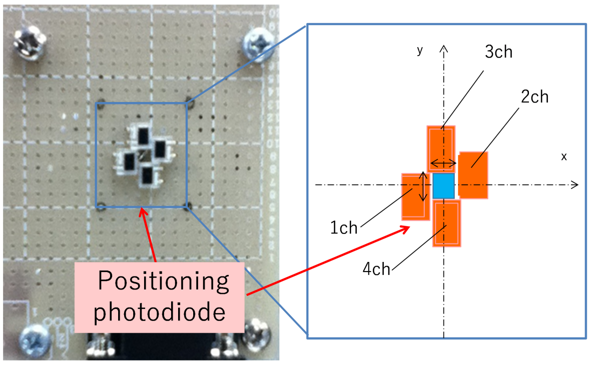

Fig. 5. Positioning photodiode set.

port Corporation) whose beam diameter, numeric aperture, beam divergence, and insertion loss, are 5.5 mm, 0.13, less than 0.25, and 0.15 dB, respectively. Laser beam is generated for positioning by a fiber-coupled Fabry-Perot laser source, S1FC980 (Thorlabs Inc.) whose wavelength and output power are 980 nm, 13 mW, respectively, and whose laser beam is precisely coupled to a single-mode pigtail fiber.

The positioning photodiode set consists of several large area Si PIN photodiodes, S8729-10 (Hamamatsu Photonics K.K.) whose spectral response range, photosensitivity, cutoff frequency, and photosensitive area are 320 to 1100 nm, 0.55 A/W, 25 MHz, and 2 mm x 3 mm, respectively.

Because these photodiodes are assembled on a printed circuit board, various arrangement of positioning photodiodes can be realized whereas interval between photodiodes is fixed.

III. Identification of Laser Optical Axis

The proposed system searches for the line-of-sight of the laser beam, and adjusts the arrived laser beam to the receiver. It is necessary to identify the optical axis of the laser beam. In case the laser intensity distribution pattern is hypothesized, optical axis position of the laser beam is conjectured from intensity data detected by several interspersed photodiodes.

A. Estimation based on four photodiodes of centrosymmetric sensitivity

If the laser beam corresponds to Gaussian beam optics, it is possible to analytically estimate the peak of the distribution. That means we can adjust the optical axis of the laser beam just onto the receiver.

Let us assume the formulation of the laser beam in the x-y-z coordinate system, providing the optical axis is parallel to the z-axis. Gaussian beam optics claims that laser beam intensity forms a point symmetry distribution.

If the center of the arrived laser beam is located at (a, b) on the x-y plane, the optical intensity, $E(x, y; E_0, w, a, b)$ of a Gaussian beam at (x, y) on the x-y plane is theoretically formulated [35] as:

$$E(x, y; E_0, w, a, b) = E_0 \exp\left(-\frac{(x-a)^2 + (y-b)^2}{w^2}\right), \tag{1}$$

where E_0 and w are the maximum intensity which is observed on the optical axis (a, b), and the radius at which the amplitude is 1/e of its value on the axis, respectively.

By locating the positioning photodiode at (x_0, y_0), we obtain the laser luminescence intensity, E_{x0y0} at that point. Then equation (1) gives the following equation:

$$(x-a)^2 + (y+b)^2 = -w^2 \log \frac{E_{x0y0}}{E_0}. \tag{2}$$

Because this equation contains four unknown parameters, E_0, w, a, b, four independent conditions are necessary to solve the simultaneous equations in general. If we have four laser luminescence intensities, E_1, E_2, E_3, E_4, of four positioning photodiodes at (x_1, y_1), (x_2, y_2), (x_3, y_3), (x_4, y_4), respectively, we obtain the optical axis (a, b) of the laser spot by solving such four simultaneous equations in terms of four variables as:

$$\begin{cases} E(x_1, y_1; E_0, w, a, b) = E_1 \\ E(x_2, y_2; E_0, w, a, b) = E_2 \\ E(x_3, y_3; E_0, w, a, b) = E_3 \\ E(x_4, y_4; E_0, w, a, b) = E_4. \end{cases} \tag{3}$$

These equations can be solved on condition that all the equations are independent.

We have examined case studies with respect to four arrangement patterns of positioning photodiode sets composed of four photodiodes as shown in Fig. 6, where parameter, k stands for the interval between neighboring photodiodes.

Let us take an example of pattern I in Fig. 6. Because positions of each photodiode, (x_1, y_1), (x_2, y_2), (x_3, y_3), (x_4, y_4), are replaced by (x, y), $(x, y+k)$, $(x+2k, y+k)$, $(x+k, y+2k)$,

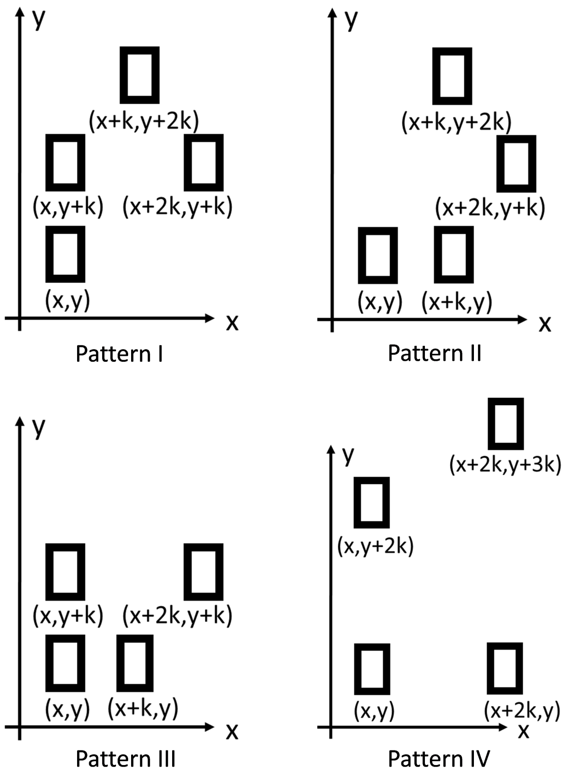

Fig. 6. Layout pattern of four positioning photodiodes.

respectively in this positioning photodiode set, we can solve the simultaneous equations and obtain the position (a, b) of the optical axis as:

$$a = \frac{(2x+3k)\log\frac{e_1}{e_4} - 4(x+k)\log\frac{e_1}{e_3} + (6x+5k)\log\frac{e_1}{e_2}}{2\log\frac{e_1}{e_4} - 4\log\frac{e_1}{e_3} + 6\log\frac{e_1}{e_2}}, \tag{4}$$

$$b = \frac{(2y+k)\log\frac{e_1}{e_4} - 2(2y+k)\log\frac{e_1}{e_3} + (6y+5k)\log\frac{e_1}{e_2}}{2\log\frac{e_1}{e_4} - 4\log\frac{e_1}{e_3} + 6\log\frac{e_1}{e_2}}, \tag{5}$$

where e_1, e_2, e_3, e_4 express the output voltages of PD1, PD2, PD3, PD4, respectively.

When a positioning photodiode set is placed at a certain position that is represented by the position (x, y) of the primacy photodiode among four, the intensity of distributed laser beam is evaluated at each point of photodiodes as output voltage, E_1, E_2, E_3, E_4. Substitution of those values into (4) and (5) yields the coordinates of the optical axis estimated based on the photodiode set at that point. By tracing all over the scanning area with the photodiode set, the optical axis position is evaluated in terms of everywhere on the plane.

We have conducted some experiments to evaluate position presumption of the optical axis. While keeping the laser beam firmly hit at the origin of coordinates, we scan around to take the laser intensity distribution, and get the output voltage of a photodiode at every point. Substitution of the measured values in the above equations gives us estimated coordinate (a, b) of the optical axis based on output voltages of the photodiodes.

Figure 7 represents estimation error maps in gray scale with regard to four patterns of positioning photodiode sets illustrated in Fig. 6. The horizontal and vertical axes denote the position of the photodiode set, whereas the actual optical axis is on the origin. This figure consists of 100 x 100 gray-scale points. Each of them indicates the estimation error when shifting the positioning photodiode set position. The shade

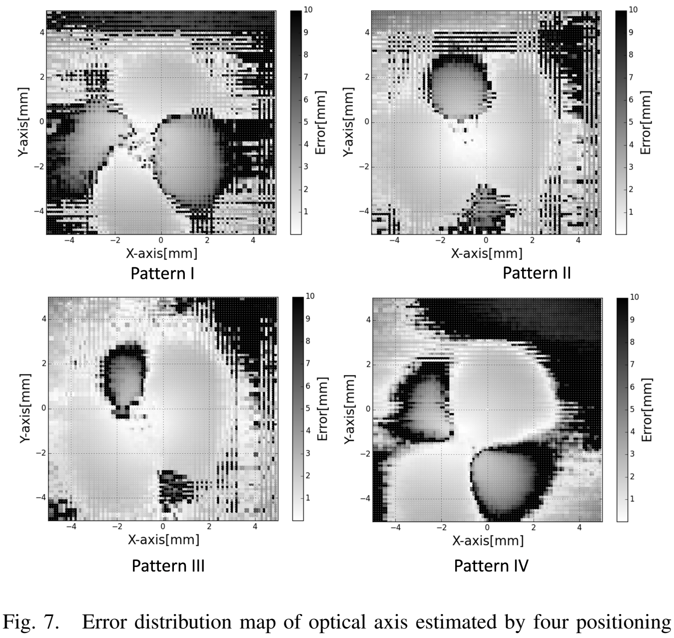

Fig. 7. Error distribution map of optical axis estimated by four positioning photodiodes.

of a point (x, y) expresses the estimation error when each photodiode pattern is just located at that position. If the laser beam luminescence were subject to the Gaussian beam optics, the luminescence estimation error would be theoretically zero at any point using any photodiode arrangement pattern. In reality, experimental results disclose that measurement errors cause some estimation error and variety of shade patterns. As for Pattern I in Fig. 6, for example, estimation error of the optical axis is less than 1 mm if the photodiode set is just on the origin, and it is 1.09 mm if the set is located at (-2.0 mm, -2.0 mm). The average of estimation is 4.7 mm within 10 mm x 10 mm according to the analytical solution by four photodiodes.

Let us investigate the estimation in detail regarding Pattern I in Fig. 7. Each point of this map denotes a Euclidean distance between the true and estimated coordinates of optical axis based on measurement with the photodiodes pattern I. When the primacy photodiode, PD1 was placed at (-2.0 mm, -2.0 mm), five photodiodes, PD1, PD2, PD3, PD4 measured each local luminescent intensity as 6.41, 6.59, 6.70, 6.71 V, respectively. By putting those values into (4) and (5), we obtained the estimated coordinates (a, b) of optical axis as (-0.76 mm, -0.78 mm). After all, a Euclidean distance between the estimated (-0.76 mm, -0.78 mm) and true coordinates (0.0 mm, 0.0 mm) of optical axis was calculated as 1.09 mm. Thus, the point (-2.0 mm, -2.0 mm) is painted by the gray scale corresponding to the Euclidean distance in Fig. 7. A number of error values were calculated in the same manner and are indicated altogether in this figure, while the photodiodes scanned over a square of 10 mm x 10 mm.

Next, the estimation accuracy is evaluated regarding Pattern I as shown in Fig. 8, while scanning area is changed to 10, 6 and 2 mm square, and photodiode interval is to 0.2, 0.5, 1.0 and 2.0 mm. The scanning area is confined if we can practically predict the possibility of the arrival point of the laser beam. The photodiode interval is related to the total size of the positioning sensor.

Average error of each case is calculated in optical axis estimation with respect to each photodiode interval, and the relationship between the area and estimation error is indicated in Fig. 9. Results verify that the averaged estimation error is lower if scanning area is smaller. It means the optical axis can be precisely identified when possible area of arrived laser beam is closely restricted.

By changing value of photodiode interval, k, we can control the gap among four photodiodes with the similar arrangement. Error patterns look different depending on the value of gap as shown in Fig. 8. Figure 10 represents the relationship between the photodiode interval and average error. Narrower photodiode interval brings a compact photodiode arrangement and results support that serried sensor can expect better resolution of estimation. For example, optical axis position is expected to be identified in an accuracy of 1.5 mm when photodiode interval is 0.5 mm and scanning within 4 mm^2.

We have investigated estimation results in the same way with respect to the other patterns of photodiode arrangement illustrated in Fig. 8. Experiments reveal the relationship between the scanning area and estimation error concerning

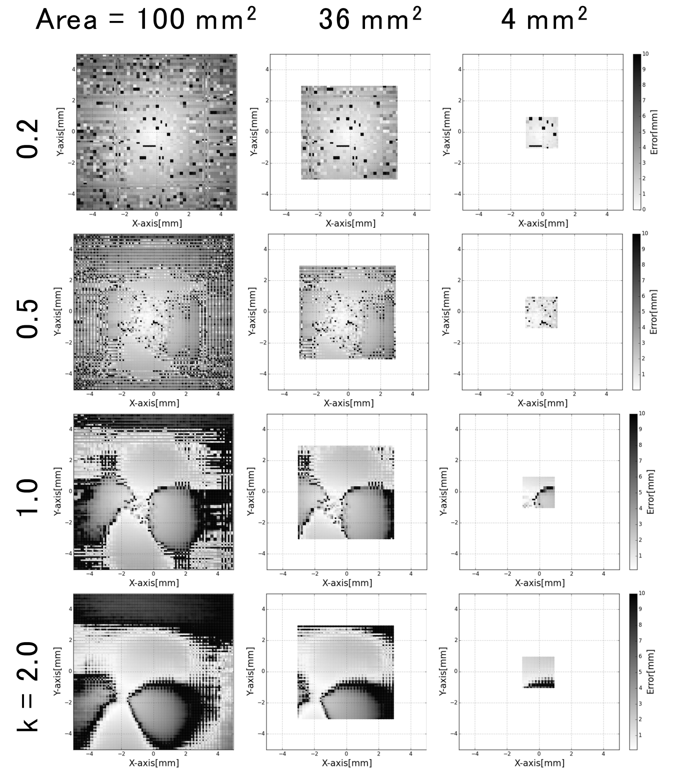

Fig. 8. Estimation error distribution with four photodiodes in terms of scanning area and photodiode interval.

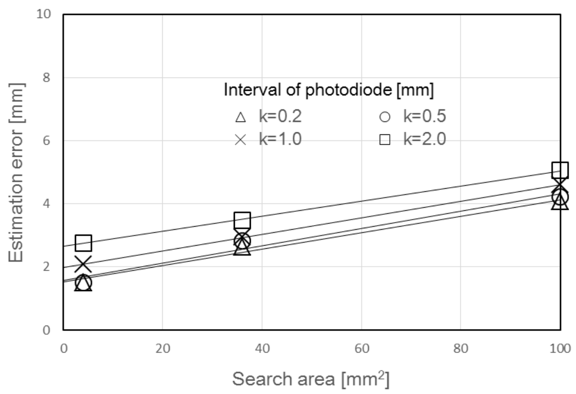

Fig. 9. Relationship between scanning area and estimation error with four photodiodes.

four different photodiode arrangements, and suggest that the arrangement pattern has small influence on the estimation results and that the estimation error is in proportion to the scanning area by using any arrangement pattern.

B. Estimation based on five photodiodes of axial- symmetric sensitivity

The practical laser intensity data measured by scanning one photodiode is indicated in Fig. 11. This signifies that the photodiode gives no concentric intensity in spite of Gaussian distribution of laser beam. Assuming that a rectangular sensitive area of the photodiode affects the output pattern, we have tried integrating of the Gaussian distribution with respect to

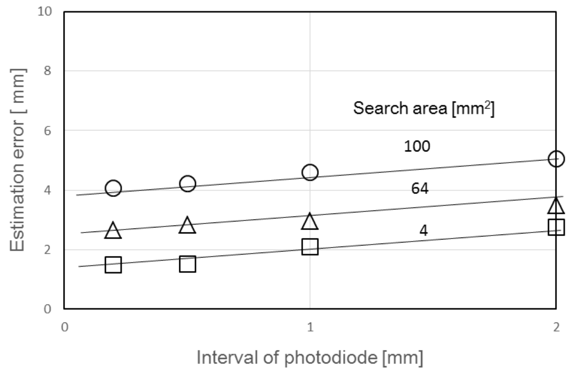

Fig. 10. Relationship between photodiode interval and estimation error with four photodiodes.

the sensitive area by (6) and confirmed that the result is similar to Fig. 11:

$$E(x,y) = E_0 \int_{b-\frac{N}{2}}^{b+\frac{N}{2}} \int_{a-\frac{N}{2}}^{a+\frac{N}{2}} \exp\left(-\frac{(x-t)^2+(y-u)^2}{w^2}\right) \mathrm{d}t\mathrm{d}u \tag{6}$$

Thus we have assumed such modified two-dimensional normal distribution as (7), and conduct the same parameter estimation using least square method:

$$E(x,y;E_0,n,m,a,b) = E_0 \exp\left(-\frac{(x-a)^2}{n^2} - \frac{(y-b)^2}{m^2}\right), \tag{7}$$

where E and E_0 represent laser intensity at (x, y) and on the optical axis, respectively. Parameters, a and b denote x- and y-coordinate of the optical axis, and n, m are the standard deviations of the x- and y-direction. Intensity, E is actually measured by the positioning photodiodes and evaluated by output voltage.

Because this equation contains five unknown parameters, E_0, n, m, a, b, five independent conditions are necessary to solve the simultaneous equation. If we have five laser luminescence intensities, E_1, E_2, E_3, E_4, E_5 of five positioning photodiodes at (x_1, y_1), (x_2, y_2), (x_3, y_3), (x_4, y_4), (x_5, y_5),

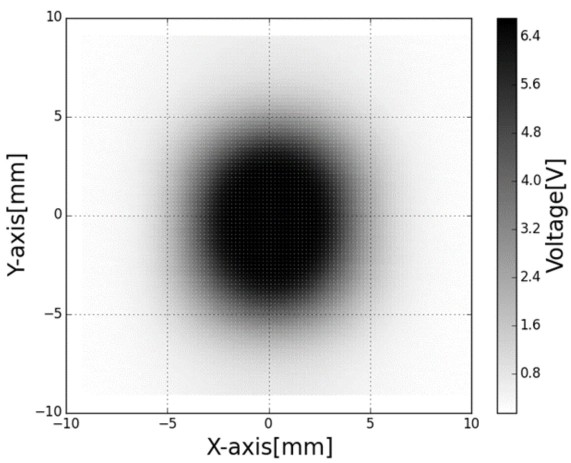

Fig. 11. Measured intensity distribution of laser spot.

respectively, we get the optical axis (a, b) of the laser spot by solving such fiver simultaneous equations in terms of fiver variables as:

$$\begin{cases} E(x_1, y_1; E_0, w, a, b) = E_1 \\ E(x_2, y_2; E_0, w, a, b) = E_2 \\ E(x_3, y_3; E_0, w, a, b) = E_3 \\ E(x_4, y_4; E_0, w, a, b) = E_4 \\ E(x_5, y_5; E_0, w, a, b) = E_5. \end{cases} \quad (8)$$

Solution of simultaneous equations with respect to laser intensity of scattered measuring points analytically provides us the coordinate (a, b) of the optical axis according to the modified Gaussian beam optics.

We have also designed some positioning photodiode sets containing five positioning photodiodes as shown in Fig. 12. We can solve the simultaneous equations of five unknown parameters concerning those layouts of photodiodes. As for Pattern I in Fig. 12, we put the data sets with respect to photodiodes PD1, PD2, PD3, PD4, PD5 be (x, y, e_1), $(x+k, y, e_2)$, $(x, y+k, e_3)$, $(x+2k, y+k, e_4)$, $(x+k, y+2k, e_5)$, respectively, where the first two elements represent x- and y-coordinates of each photodiode, and the last element denotes photodiode voltage expressing laser intensity. Parameter, k, stands for the interval between neighboring photodiodes. Total area of the positioning sensor can be altered by the value of k while maintaining the photodiode configuration similar.

Eventually, we obtain coordinate (a, b) of the optical axis as follows:

$$a = \frac{4(x+k)\log\frac{e_1}{e_5} + (2x+k)\log\frac{e_4}{e_2}}{4\log\frac{e_1}{e_5} + 2\log\frac{e_4}{e_2}}, \quad (9)$$

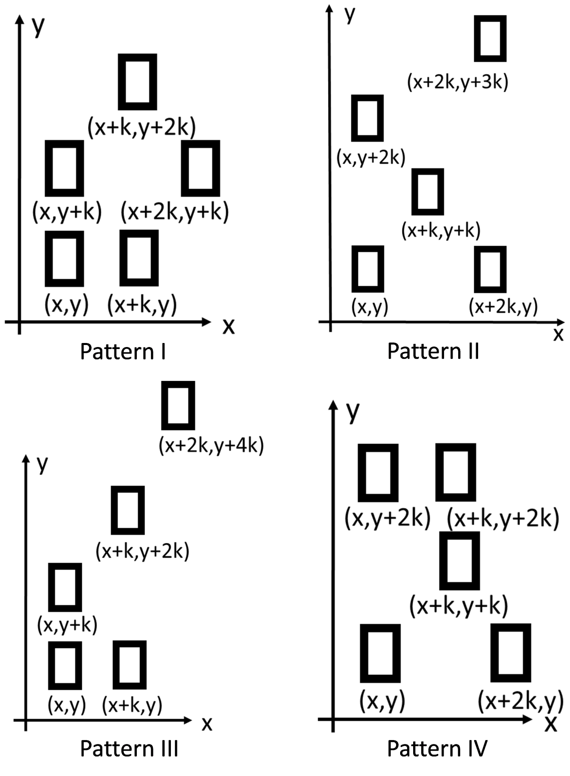

Fig. 12. Layout pattern of five positioning photodiodes.

$$b = \frac{(2y+k)\log\frac{e_5}{e_3} + 4(y+k)\log\frac{e_2}{e_1}}{2\log\frac{e_5}{e_3} + 4\log\frac{e_2}{e_1}}. \quad (10)$$

Fundamental experiments are carried out by applying the analysis. Distribution of the laser beam intensity is actually measured by those five positioning photodiodes. The optical axis position is estimated based on the measured intensity of the photodiodes. By scanning the photodiode set on a plane vertical to the optical axis, we obtain the estimation values at every position of the photodiode set as shown in Fig. 13. This figure illustrates the presumption error distribution map displayed by gray scale, where shade of a point (x, y) represents the presumption error value when the photodiode set is placed at coordinates (x, y).

Focusing on one of results in Fig. 13, the upper left chart displays errors of optical axis coordinates estimated using positioning photodiode set, Pattern I under the condition that photodiode interval is 1.0 mm and search area is 100 mm^2. Each point within the area stands for a Euclidean distance between the estimated and true coordinates of optical axis. When the primacy photodiode, PD1 is placed at (-2.0 mm, -2.0 mm), five photodiodes, PD1, PD2, PD3, PD4, PD5 measure each local luminescent intensity as 6.41, 6.59, 6.70, 6.71, 6.68 V, respectively. By substituting these values into (9) and (10), we obtain the estimated coordinates (a, b) of optical axis as (-0.97 mm, -0.97 mm). Consequently, a Euclidean distance between the estimated coordinates (-0.97 mm, -0.97 mm) and true coordinates (0.0 mm, 0.0 mm) of optical axis is calculated as 1.38 mm. Thus, the point (-2.0 mm, -2.0 mm) of the chart in Fig. 13 expresses the value of presumption error by gray scale. Numerous error values are evaluated in the same way and are indicated altogether in this chart while the system scanned all over 100 mm^2 areas.

Next we alter the scanning area 100, 36, and 4 mm^2, and obtained estimation accuracy as shown in Fig. 14 with regard

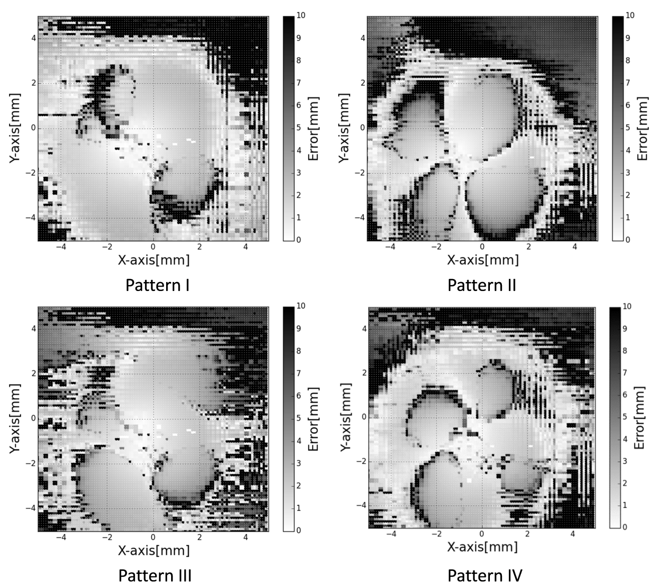

Fig. 13. Error distribution map of optical axis estimated by five positioning photodiodes.

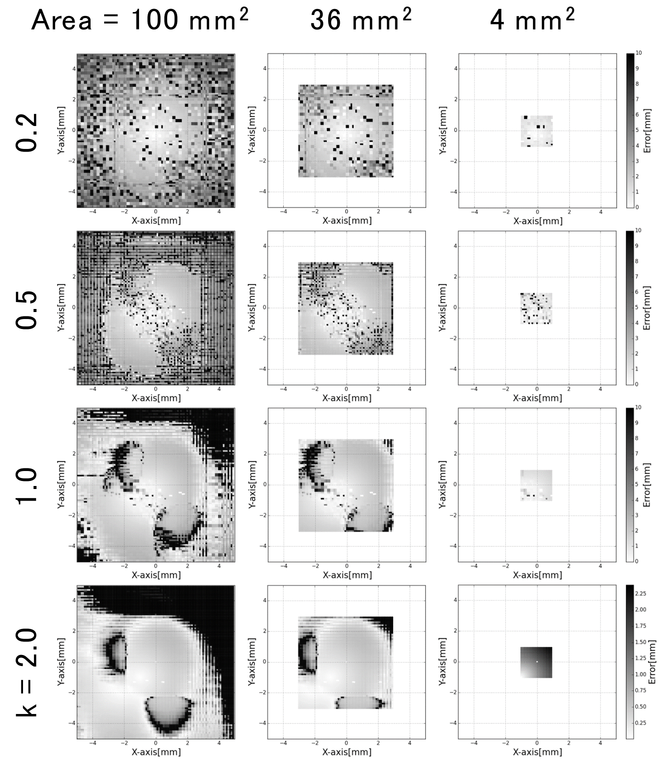

Fig. 14. Estimation error distribution with five photodiodes in terms of scanning area and photodiode interval.

to several values of photodiode interval, k as 0.2, 0.5, 1.0, and 2.0 mm. Bigger photodiode interval provides us large sensitive area of positioning sensor. Position sensor size is considered to be related also to measurement accuracy.

Average estimation error of optical axis is calculated at several scanning areas. Figure 15 represents the relationship between the search area and estimation error. Results disclose that the averaged estimation error is approximately proportional to the search area, and it is independent of the photodiode intervals. For example, the accuracy to identify optical axis position is around 1.0 mm when photodiode interval is 0.5 mm and searching area is 4 mm^2. It suggests that we can choose smaller interval to obtain fine resolution of position measurement using compact positioning sensor if arrival point of the laser beam is restricted.

We can use the similar arrangement of positioning sensor containing five photodiodes by selecting the value of parameter, k. The relationship between the photodiode interval and average estimation error is indicated in Fig. 16. The interval is related to sensor size, and results support that the sensor size has little effect on the accuracy of estimation for any size of scanning area.

IV. Conclusion

This paper describes the optical axis adjustment technique for active free space optics. The laser beam transmission system is designed and prototyped first. We propose the position estimation method of the laser beam optical axis next. Gaussian beam optics is modified and it provides the analytical formulation of the laser beam optical axis to determine laser

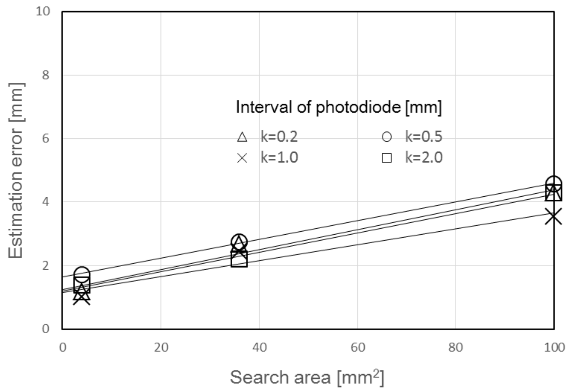

Fig. 15. Relationship between scanning area and estimation error with five photodiodes.

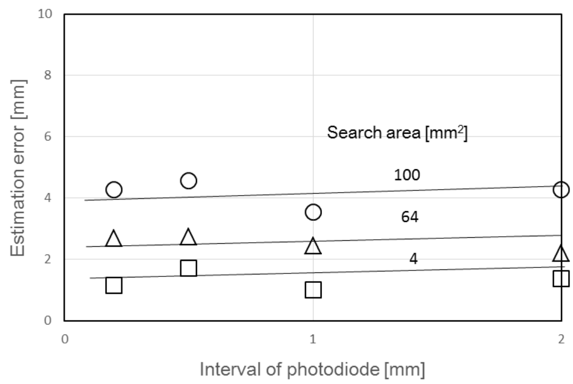

Fig. 16. Relationship between photodiode interval and estimation error with five photodiodes.

arrival point. It enables us to presume the scattered laser distribution based on several sampling data of local lase intensity. We have investigated both cases when the photodiode sensitivity is centrosymmetric and axial-symmetric. In the former case, Gaussian beam optics theory is applied to formulate the optical axis estimation, which uses only four photodiodes. As for the latter, the modified Gaussian beam optics helps us to establish presumption of laser position based on five photodiodes. Some experiments are carried out to identify optical axis position with respect to several sensor layouts and sensitive areas. Results disclose that estimation error is mainly related to scanning area, and the experimental setup which contains only four or five photodiodes determines the laser spot in an accuracy of around 1 mm. This paper has proved that the proposed method is available for primary alignment of free space optics laser transmission.

References

[1] H. Willebrand, and B. S. Ghuman, *Free-Space Optics: Enabling Optical Connectivity in Today's Networks*, Sams Publishing, 1999.

[2] D. C. O'Brien, G. Faulkner, E. B. Zyambo, and K. Jim, Integrated transceivers for optical wireless communications, *IEEE J. Selected Topics in Quantum Electronics*, vol. 11, no. 1, pp. 173-183, 2005.

[3] J. Vitasek, E. Leitgeb, T. David, and J. Latal, Misalignment loss of Free Space Optic link, in *Proc. 16th Int. Conf. Transparent Optical Networks*, pp. 1-5, 2014.

[4] S. Dubey, S. Kumar, and R. Mishra, Simulation and performance evaluation of free space optic transmission system, in *Proc. Int. Conf. Computing for Sustainable Global Development*, pp. 850-855, 2014.

[5] P. Puri, P. Garg, and M. Aggarwal, Partial Dual-Relay Selection Protocols in Two-Way Relayed FSO Networks, *J. Lightwave Technology*, vol. 33, no. 21, pp. 4457-4463, 2015.

[6] P. Puri, N. D. Chatzidiamantis, P. Garg, M. Aggarwal, and G. K. Karagiannidis, Two-Way Relay Selection in Multiple Relayed FSO Networks, *IEEE Wireless Communications Letters*, vol. 4, no. 5, pp. 485-488, 2015.

[7] J. Xue, A. Garg, B. Ciftcioglu, S. Wang, J. Hu, I. Savidis, M. Jain, M. Huang, H. Wu, E. G. Friedman, G. W. Wicks, D. Moore, An intrachip free-space optical interconnect, in *Proc. 37th annual international symposium on Computer architecture*, pp. 94-105, 2010.

[8] A. Gomez, K. Shi, C. Quintana, G. Faulkner, B. C. Thomsen, and D. OBrien, A 50 Gb/s Transparent Indoor Optical Wireless Communications Link With an Integrated Localization and Tracking System, *Journal of Lightwave Technology*, vol. 34, no. 10, pp. 2510-2517, 2016.

[9] A. Sharma, and R.S. Kaler, Designing of high-speed inter-building connectivity by free space optical link with radio frequency backup, *IET Communications*, vol. 6, no. 16, pp. 2568-2574, 2012.

[10] R. Brning, B. Ndagano, M. McLaren, S. Schrter, J. Kobelke, M. Duparr and A. Forbes, Data transmission with twisted light through a free-space to fiber optical communication link, *Journal of Optics*, vol. 18, no. 3, 03LT01, 2016.

[11] H. Kaushal, G. Kaddoum, V. K. Jain, and S. Kar, Experimental investigation of optical beam size for FSP uplink, *Optics Communications*, vol. 400, pp. 106-114, 2017.

[12] K. Tanaka, T. Tsujimura, K. Yoshida, K. Katayama, and Y. Azuma, Frame-loss-free Line Switching Method for In-service Optical Access Network using Interferometry Line Length Measurement, in *Proc. Optical Fiber Communication Conf. and National Fiber Optic Engineers Conf.*, postdeadline PDPD6, 2009.

[13] M. Taheri, N. Ansari, J. Feng, R. R-Cessa, and M. Zhou, Provisioning Internet Access Using FSO in High-Speed Rail Networks, *IEEE Network*, vol. PP, no. 99, pp. 12-17, 2017.

[14] Y. L. Yu, S. K. Liaw, H. H. Chou, H. L. Minh, and Z. Ghassemlooy, A Hybrid Optical Fiber and FSO System for Bidirectional Communications Used in Bridges, *IEEE Photonics Journal*, vol. 7, no. 6, No. 7905509, 2015.

[15] S. K. Liaw, K. Y. Hsu, J. G. Yeh, and Y. L. Yu, Impacts of environmental factors to bi-directional 240 Gb/s WDM free-space optical communication, *Optics Communications*, vol. 396, pp. 127-133, 2017.

[16] N. A. M. Nor, Z. F. Ghassemlooy, J. Bohata, P. Saxena, M. Komanec, S. Zvanovec, M. R. Bhatnagar, and M. A. Khalighi, Experimental Investigation of All-Optical Relay-Assisted 10 Gb/s FSO Link Over the Atmospheric Turbulence Channel, *Journal of Lightwave Technology*, vol. 35, no. 1, pp. 45-53, 2017.

[17] N. Badar, and R. K. Jha, Performance comparison of various modulation schemes over free space optical (FSO) link employing GammaGamma fading model, *Optical and Quantum Electronics*, vol. 49, no. 192, 2017.

[18] M. A. Esmail, H. Fathallah, and M. S. Alouini, Outdoor FSO Communications Under Fog: Attenuation Modeling and Performance Evaluation, *IEEE Photonics Journal*, vol. 8, no. 4, 2016.

[19] M. H. Ibrahim, H. A. Shaban, and M. H. Aly, Effect of different weather conditions on BER performance of single-channel free space optical links, *Optik - International Journal for Light and Electron Optics*, vol. 137, pp. 291-297, 2017.

[20] M. P. Nicos, H. E. Nistazakis, and G. S. Tombras, On the BER performance of FSO links with multiple receivers and spatial jitter over gamma-gamma or exponential turbulence channels, *Optik - International Journal for Light and Electron Optics*, vol. 138, pp. 269-279, 2017.

[21] F. Zhu, S. Huang, W. Shao, J. Zhang, M. Chen, W. Zhang, and J. Zeng, Free-space optical communication link using perfect vortex beams carrying orbital angular momentum (OAM), *Optics Communications*, vol. 396 , pp. 50-57, 2017.

[22] D. Zheng, Y. Li, B. Li, W. Li, E. Chen, and J. Wu, Free Space to Few-Mode Fiber Coupling Efficiency improvement with Adaptive Optics under Atmospheric Turbulence, in *Proc. 2017 Optical Fiber Communication Conference*, pp. 1-3, 2017.

[23] Z. Huang, Z. Wang, M. Huang, W. Li, T. Lin, P. He, and Y. Ji, Hybrid Optical Wireless Network for Future SAGO-Integrated Communication Based on FSO/VLC Heterogeneous Interconnection, *IEEE Photonics Journal*, vol. 9, no. 2, pp. 7902410, 2017.

[24] Y. Sun, F. Yang, and J. Gao, Comparison of Hybrid Optical Modulation Schemes for Visible Light Communication, *IEEE Photonics Journal*, vol. 9, no. 3, pp. 7904213, 2017.

[25] Z. Jing, Z. Shang-hong, Z. Wei-hu, and C. Ke-fan, Performance analysis for mixed FSO/RF Nakagami-m and Exponentiated Weibull dual-hop airborne systems, *Optics Communications*, vol. 392, pp. 294-299, 2017.

[26] T. Rakia, F. Gebali, H. C. Yang, and M. S. Alouini, Cross layer analysis of P2MP hybrid FSO/RF network, *IEEE/OSA Journal of Optical Communications and Networking*, vol. 9, no. 3, pp. 234-243, 2017.

[27] J. Park, E. Lee, C.B. Chae, and G. Yoon, Impact of Pointing Errors on the Performance of Coherent Free-Space Optical Systems, *IEEE Photonics Technology Letters*, vol. 28, no. 2, pp. 181-184, 2016.

[28] H. G. Sandalidis, N. D. Chatzidiamantis, and G. K. Karagiannidis, A Tractable Model for Turbulence- and Misalignment-Induced Fading in Optical Wireless Systems, *IEEE Communications Letters*, vol. 20, no. 9, pp. 1904-1907, 2016.

[29] L. Li, Y. Huang, Q. Wang, and F. Yang, Noise adaptive fading Kalman filter for free-space laser communication beacon tracking, *Applied Optics*, vol. 55, no. 30, pp. 8486-8493, 2016.

[30] T. Tsujimura, and K. Yoshida, Active free space optics systems for ubiquitous user networks, in *Proc. Conf. Optoelectronic and Microelectronic Materials and Devices*, pp. 197-200, 2004.

[31] K. Tanaka, T. Tsujimura, K. Yoshida, K. Katayama, and Y. Azuma, Frame-loss-free Optical Line Switching System for In-service Optical Network, *J. Lightwave Technology*, pp. 539-546, 2009.

[32] T. Tsujimura, K. Yoshida, and K. Tanaka, Length measurement for optical transmission line using interferometry, *Interferometry*, InTech, 2012.

[33] K. Yoshida, K. Tanaka, T. Tsujimura, and Y. Azuma, Assisted Focus Adjustment for Free Space Optics System Coupling Single-Mode Optical Fibers, *IEEE Trans. Industrial Electronics*, vol. 60, pp. 5306-5314, 2013.

[34] T. Tsujimura, K. Izumi, and K. Yoshida, Transmission Laser Beam Control Techniques for Active Free Space Optics Systems, *E-Business and Telecommunications*, Springer, pp.169-188, 2015.

[35] Robert D. Guenther, *Modern optics*, John Wiley & Sons. Inc., 1990.